

DTIC FILE COPY

2

AD-A226 621

TIC
ECTE
19 1990

D CS D

NAVSPASUR Direction Cosine Processing

Daniel Solomon

INTERFEROMETRICS INC.

August 31, 1990

DISTRIBUTION STATEMENT A

Approved for public release
Distribution Unlimited

Prepared for
The Naval Research Laboratory
Naval Center for Space Technology
Space Systems Engineering Department
Space Applications Branch
Under Contract N00014-87-C-2547

90 09 13 119

NAVSPASUR Direction Cosine Processing

Daniel Solomon

Abstract

This report is a description of the NAVSPASUR Operations Center process of reducing the receiver station data to local direction cosines for the (new) St. Andrew's cross stations, a configuration for which most of the antennas have their phase centers aligned along north-east and south-east directions. The following observational parameters are also determined: direction cosine rates, Doppler, and chirp

Most of the main steps involved are the same as for the older cruciform stations, whose antenna phase centers are aligned along north-south and east-west axes. This algorithm has recently been modified by the Analysis and Software Department of NAVSPASUR for use with the St. Andrew's cross configuration. The direction cosine algorithm uses a walkup and least squares as before, but differs due to the antenna configuration. Those modifications were in effect by January 1, 1990, the *freeze date* for this report. It is hoped that the present report will elucidate the NAVSPASUR direction cosine processing for the surveillance community. A detailed error analysis of the steps involved in the direction cosine determination processing is in progress and will be issued eventually. Most of the present report will be incorporated into a longer one describing the NAVSPASUR Operations Center process of satellite element updates.

Approved by:	
NTIS	✓
DTIC	✓
Understand	✓
Justification:	
By <i>per call</i>	
Distribution:	
Availability Codes	
Dist	Availability for Special
A-1	



Approved by:

Carl J. Morris
Carl J. Morris, COTR

Date: 9/4/90

STATEMENT "A" per Carl Morris
NRL/Code 83241
TELECON

9/17/90

VC

Contents

Introduction	1
1 Principles of Interferometry	7
2 Data Format	10
3 The Observation Time	14
4 Cosine Rates and Smoothed Phases	15
5 Direction Cosines	20
6 Doppler and Chirp	28
Acknowledgements	29
A Least Squares	30
References	31

List of Figures

1	Map of NAVSPASUR facilities	1
2	NAVSPASUR Operations Center data processing	2
3	Typical low altitude Cruciform station configuration (not to scale)	3
4	Low altitude St. Andrew's cross station configuration	4
5	Direction cosine processing overview	6
6	Two-element interferometer	7
7	Near field interferometer effects	8
8	Schematic of data from one antenna	10
9	The phase error in the receiver software in counts, for $0 \leq \tan^{-1} y/x \leq \pi/2$. .	12
10	The weighting function of frame amplitude	15
11	Flow chart summary of phase smoothing and cosine rates.	16
12	Flow chart summary of direction cosine resolution	24

List of Tables

1	Typical satellite pass.	13
2	St. Andrew's cross baselines	22
3	Antenna pairs used to create baselines	25

Introduction

The NAVSPASUR sensor is a multistatic continuous wave radar system with nine stations (three transmitters and six receivers) located along a great circle path, inclined 33.57 degrees to the equator across the southern United States, (see Fig. 1). The main transmitter is at the Kickapoo Lake Station, and the wing transmitters are at Wetumpka and Gila River. The transmitters broadcast fan-shaped beams at 216.98 MHz, and the unsynchronized beams combine to form the NAVSPASUR *fence*, which is very narrow in the north-south direction, but very wide in the east-west direction. When an object such as a satellite enters the fence a small fraction of the transmitted radio energy is reflected to one or more of the receiver sites. Interferometric techniques are applied to determine the angles of arrival of the reflected signal at each receiving station.

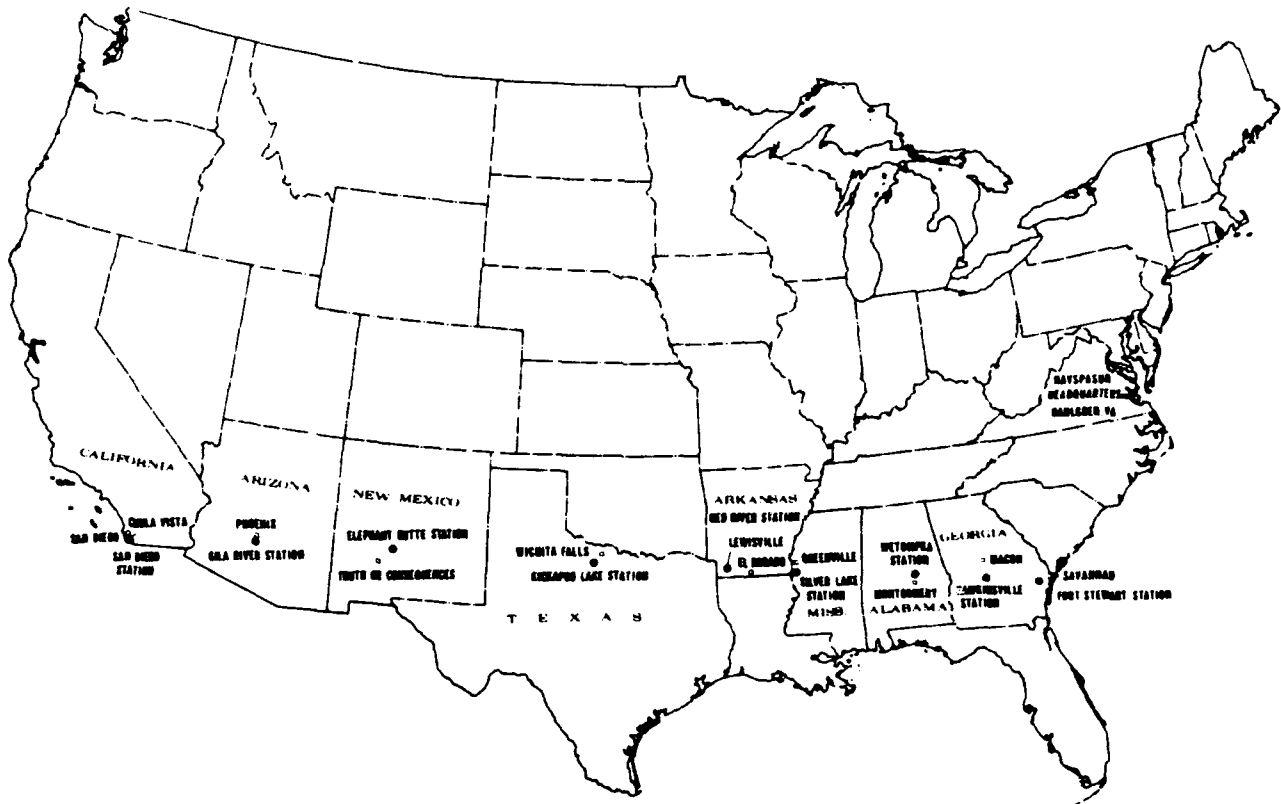


Figure 1: Map of NAVSPASUR facilities

The data from all receivers are collected in real time and fed via dedicated telephone lines directly into the central data processing system at the NAVSPASUR Operations Center in Dahlgren, Virginia. At the Operations Center data from each receiving station is reduced

to local direction cosines for each object, along with cosine rates, Doppler and chirp, statistical measures, and time stamps. The NAVSPASUR Operations Center maintains satellite element catalogs, which are updated with the reduced data. A broad overview of the Operations Center processing is given in the flow chart of Fig. 2. The main part of this report is a detailed description of the box labeled "RESOLUTION."

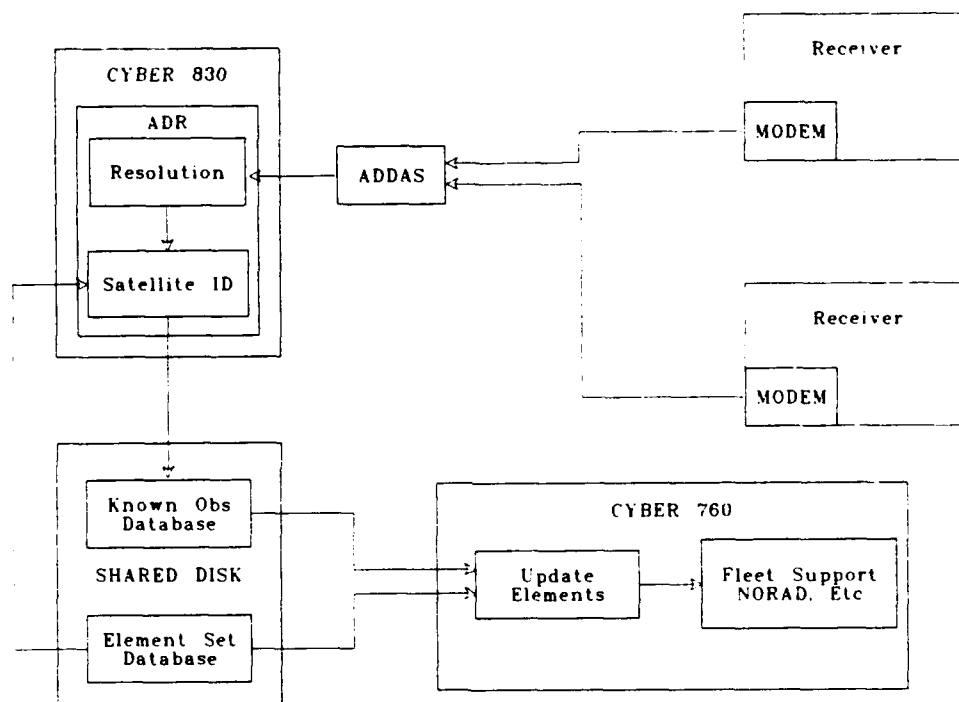
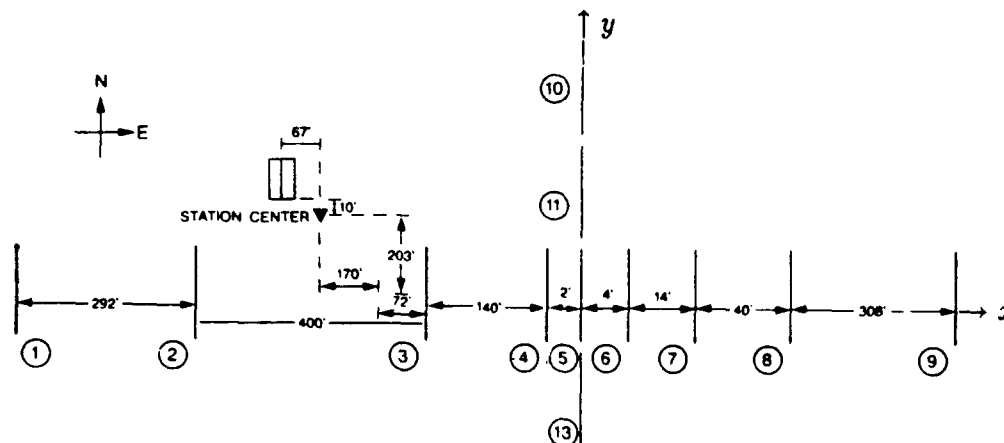


Figure 2: NAVSPASUR Operations Center data processing

The local coordinate system, called East-North-Up, is defined by its unit coordinate directions. Up (z) is in the direction of the local vertical as established with a plumb line at a point at the station, and the antennas are in a perpendicular plane, established with a laser survey. East and North coincide with the directions formed by the antenna phase centers in the cruciform array shown in Fig. 3 (not to scale). Moreover, East (x or \hat{E}) lies in the plane of the great circle and is tangent to it; North (y or \hat{N}) is perpendicular to the great circle. If a satellite is in the direction \hat{x}_s from the center of the receiving station, then the East and North *direction cosines* for the satellite are defined by $\hat{E} \cdot \hat{x}_s$ and $\hat{N} \cdot \hat{x}_s$, respectively. These quantities are the cosines of the angles formed by \hat{x}_s and the coordinate axes, and are the fundamental observation parameters used.



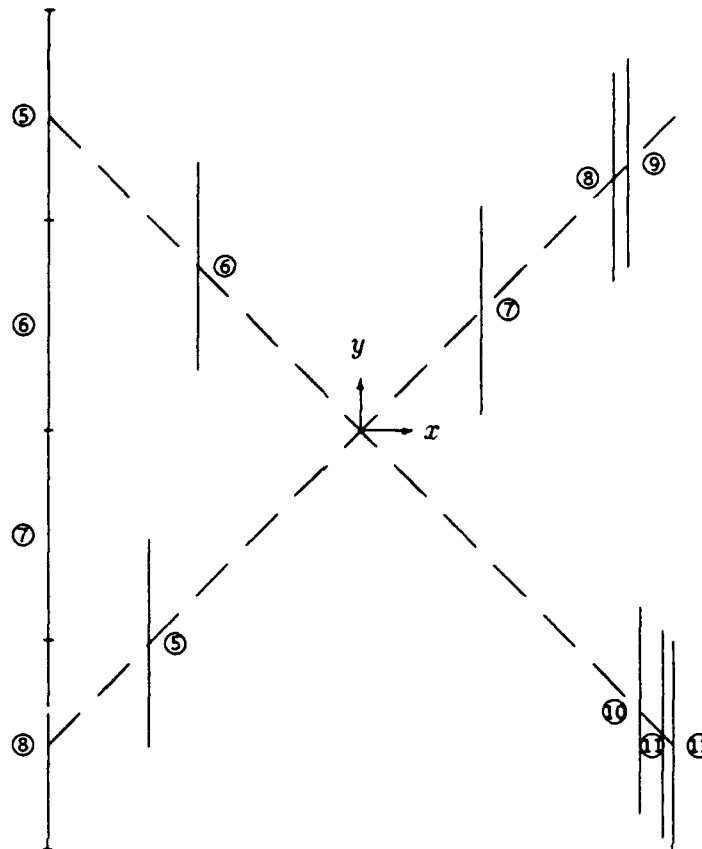
Antenna Coordinates in Feet Relative to Reference Point												
	1	2	3	4	5	6	7	8	9	10	11	13
<i>x</i>	-834	-542	-142	-2	0	4	18	58	366	0	0	0
<i>y</i>	0	0	0	0	0	0	0	0	0	800	400	-400

Figure 3: Typical low altitude Cruciform station configuration (not to scale)

The physical deployment of the antennas is intended to allow for the unambiguous determination of direction cosines from the station to the satellite. The antennas are configured as an array of collinear half-wave dipoles and are positioned to form interferometric base-lines of varying lengths. For each antenna the radio frequency (RF) signals from all of the dipoles are combined coherently (since the antennas are in a plane) and directed through an analog filter into a preamplifier. The filters are designed to remove specific signals from local transmissions and do not exist at all sites.

Four of the receiving stations are intended for detecting low altitude satellites, and the other two are for high altitude satellites. NAVSPASUR has recently undertaken a program to convert the antenna array configuration from the cruciform to the St. Andrew's cross. The low altitude St. Andrew's cross stations are illustrated in Fig. 4. They are composed of twelve antennas 400 feet long. The high altitude stations are composed of ten antennas each 2400 feet long. The antenna configurations for low and high altitude differ only in the lack of antennas 2 and 3 at the high altitude stations. Antennas 1 and 4 overlap by 1200 feet in the high altitude stations. We shall use the name N_a to mean the number of antennas at the receiving station under consideration (ten or twelve).

The fundamental quantity measured by the NAVSPASUR sensor system is the set of signal phases received at each antenna at a given receiving station. The raw phases from



Antenna Coordinates in Feet Relative to Reference Point												
	1	2	3	4	5	6	7	8	9	10	11	12
<i>x</i>	-600	-600	-600	-600	-406	-312	230	482	510	536	580	600
<i>y</i>	600	200	-200	-600	-406	312	230	482	510	-536	-580	-600

Figure 4: Low altitude St. Andrew's cross station configuration

each of the antennas are combined to produce phase differences, each taken with respect to the designated reference antenna. In an interferometer system these relative phases are caused by differences in the arrival times of the signal at the different antennas. The basic problem is: given the antenna layout and the measured phases, determine the satellite direction.

For a given satellite pass up to 55 *frames* of signal phases are recorded at a 54.93 Hz sample rate, allowing the determination of satellite *cosine rates*, which are time derivatives of the direction cosines. The Doppler and chirp of the received signal are also determined.

Each receiver station has a primary and secondary receiving system assuring that in the event of equipment failure the station is still able to perform in its primary mode. The primary mode is the full Doppler processing mode, which makes nearly all of the system's target detections. If only one system is operational, that system is designated the primary system. The secondary system, when available, performs in the half and quarter Doppler processing modes, which were designed to detect the fainter signals of higher altitude satellites. The pertinent details of the full Doppler processing mode will be discussed. The half and quarter Doppler processing modes and the secondary system as a whole will not be treated.

The diagonal arms of the St. Andrew's cross are at 45° angles to the east-west direction. These directions are referred to as L_1 and L_2 for northeast and southeast respectively. The direction cosines determined with respect to L_1 and L_2 are called ℓ_1 and ℓ_2 . For historical reasons east-west and north-south direction cosines are desirable. The transformation is accomplished as follows:

$$\begin{aligned} m_1 &= \frac{1}{\sqrt{2}}(\ell_1 + \ell_2) \\ m_2 &= \frac{1}{\sqrt{2}}(\ell_1 - \ell_2), \end{aligned} \tag{1}$$

where m_1 and m_2 are the east-west and north-south cosines.

Other observational parameters are determined, including the direction cosine rates, Doppler and chirp. This suite of processing is collectively referred to as *direction cosine processing*. An overview of the direction cosine processing is shown in the flowchart of Fig. 5 and may be summarized as follows:

- Choose an observation time at which to set the estimates.
- Smooth the phases and determine the direction cosine rates with least squares.
- Determine the direction cosines with walk up and least squares.
- Determine the Doppler and chirp with an FFT and least squares.

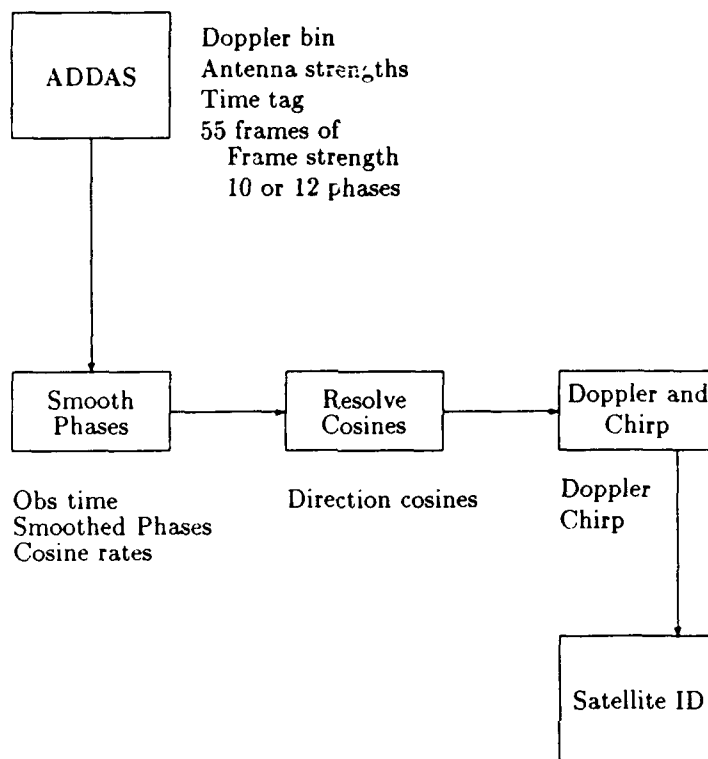


Figure 5: Direction cosine processing overview

Section 1 is an overview discussion of the principles of interferometry including an estimate showing that the receiver interferometer near field effects on antenna phase do not cause significant errors in the direction cosine determinations. The format of the phase data which arrives at NAVSPASUR is described in Section 2. Details on the observation time are in Section 3. Smoothing the phase data and determining cosine rates are described in Section 4. The detailed description of the direction cosine processing is contained in Section 5. The Doppler and chirp calculation is described in Section 6. An appendix summarizes the least squares formalism. Items within square brackets refer to bibliography entries at the end.

1 Principles of Interferometry

A comprehensive description of interferometry may be found in [Kraus] and [Tho]. The simplest interferometer consists of a pair of antennas characterized by the vector from the *reference* antenna to the *remote* one. This vector \mathbf{b} is called the baseline. In the limit where the source of the radiation is infinitely distant (known as the *parallel rays assumption*), a plane-wave signal is received at each antenna with a relative phase difference which depends on the direction to the source of the radiation. This is illustrated in Fig. 6.

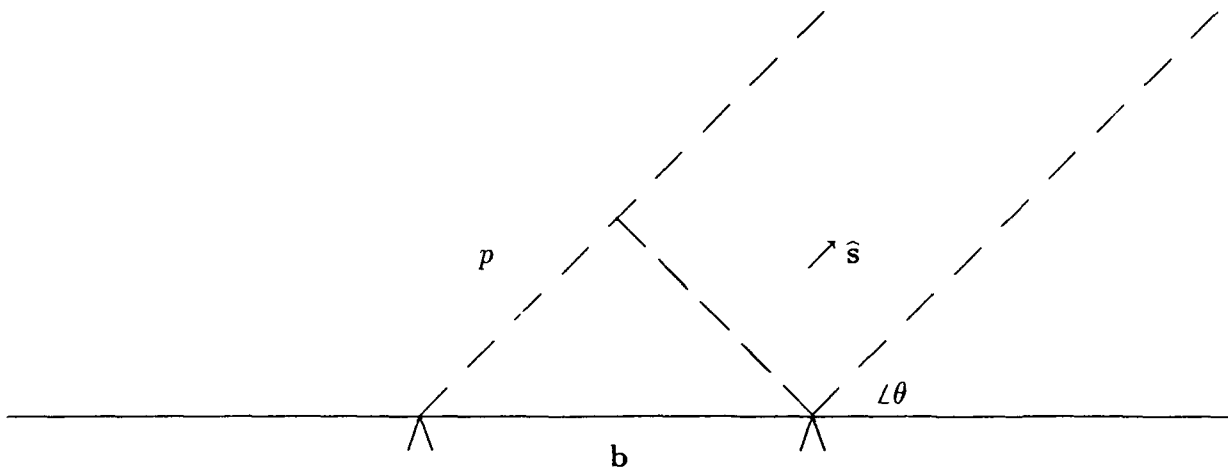


Figure 6: Two-element interferometer

The angle θ to a radiating or reflecting satellite is given by

$$\cos \theta = \hat{\mathbf{s}} \cdot \frac{\mathbf{b}}{b} = \frac{p}{b} \quad (2)$$

where $\hat{\mathbf{s}}$ is the unit vector in the direction of the satellite, $b = |\mathbf{b}|$, and p is the path length difference from the source to the two antennas. If the received voltages are expressed as v_0 and $v_1 = v_0 e^{i2\pi\phi}$, then under the assumption of parallel rays the phase difference $2\pi\phi$ between the received voltages at the antennas is $2\pi p/\lambda$, where λ is the wavelength of the received radiation. In terms of measured quantities the direction cosine is given by

$$\cos \theta = \frac{\lambda}{b} \phi. \quad (3)$$

The error in the cosine due to phase measurement error is

$$d \cos \theta = \frac{\lambda}{b} d\phi,$$

indicating that longer baselines give cosine estimates with smaller errors. On the other hand this phase difference $2\pi\phi$ is directly measured only up to a multiple of 2π . As a consequence, $\cos \theta$ is ambiguous by multiples of λ/b . This is known as the *cosine ambiguity*. If two sources were situated with direction cosines differing by λ/b , they would produce identical phase difference data on the antennas. This means it is impossible to determine from phase measurements whether a given target has a direction cosine x or $x + k\lambda/b$ for k an integer. The interferometer is also said to have *grating lobes* spaced at intervals of λ/b , although the phrase is usually reserved for ambiguities in the multi-antenna case. Direct phase difference measurement can be accomplished if the baseline is shorter than one wavelength.

As will be seen, a solution to the competing needs for short and long baselines is based on beginning with a short baseline, and applying the walkup through longer baselines. This overcomes the ambiguity and yields the intrinsic accuracy of long baselines.

The parallax effect due to the satellite being in the near field of the interferometer receivers does not cause trouble with the direction cosine estimates. Parallax arises as the error in the measured phases due to the parallel rays assumption and may be estimated with trigonometry. (See Fig. 7). Let R , R_0 , and R_1 be the slant ranges to the satellite from the center of the interferometer and the nearer and farther antennas respectively. Then

$$R_0^2 = R^2 + b^2/4 + bR \cos \theta$$

$$R_1^2 = R^2 + b^2/4 - bR \cos \theta$$

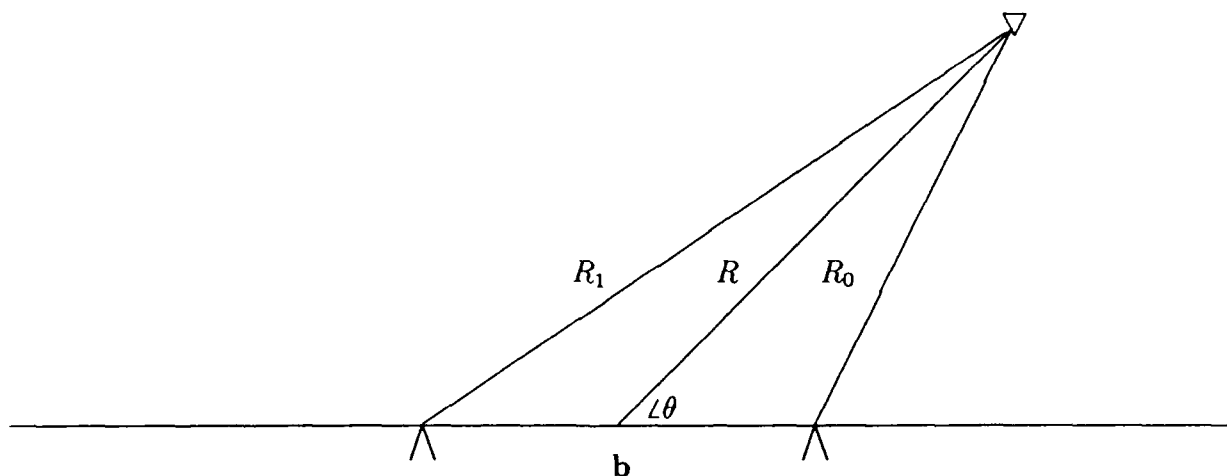


Figure 7: Near field interferometer effects

so that

$$(R_0 - R_1)/R = \sqrt{1 + \frac{b^2/4 + bR \cos \theta}{R^2}} - \sqrt{1 + \frac{b^2/4 - bR \cos \theta}{R^2}}.$$

The square roots may be approximated by an application of the binomial expansion:

$$(1+x)^{1/2} \sim 1 + \frac{1}{2}x - \frac{1}{8}x^2 + \frac{1}{16}x^3$$

which after simplifying and discarding terms of order 4 in b/R yields

$$R_0 - R_1 \sim b \cos \theta - \frac{1}{8} \frac{b^3}{R^2} \cos \theta \sin^2 \theta.$$

The estimate for $\cos \theta$ is Eq. (2):

$$\overline{\cos \theta} = \frac{R_0 - R_1}{b} \sim \cos \theta - \frac{1}{8} \frac{b^2}{R^2} \cos \theta \sin^2 \theta.$$

The random variable $\cos \theta \sin^2 \theta$ has a mean of zero and a standard deviation of $1/2\sqrt{2}$. This means the error is unbiased and has a standard deviation of $\frac{b^2}{16\sqrt{2}R^2}$, which for the case of a baseline of $1200\sqrt{2}$ feet and a satellite range of 100 km, is less than $1.2 \cdot 10^{-6}$, more than two orders of magnitude smaller than the nominal rms cosine error of 0.00025. So the parallel rays assumption is valid for all St. Andrew's cross baselines and all satellites.

2 Data Format

At the receiving stations the Interferometer Subsystem (IS) measures the complex voltages received from an object which is illuminated by one of the transmitters. Subsequent data processing (to be discussed) determines the amplitudes and phases of the signals.

The IS includes three digital filters (DFs), which are narrow band filters passing only the selected frequency component by means of a discrete Fourier transform (DFT). Tuning a DF is equivalent to selecting the frequency to be passed. For each target a particular DF is tuned to the Doppler frequency of the selected target. The tuning consists of storing the appropriate coefficients for multiplication by the sample values. Each DF receives all of the data samples from all of the antennas. The multiplexed data is received at a 1.2 MHz rate, or 75 kHz for a single antenna's data. In a particular DF, sample blocks are created consisting of 4096 consecutive samples from each antenna. Collecting 4096 samples from each antenna requires 54.61 msec. The data from each antenna is overlapped three-to-one, which means each sample becomes a member of three blocks, and one block for each antenna is completed every 18.2 msec. This is illustrated in Fig. 8. (Since 4096 is not evenly divisible by three, a new block is started after each of two consecutive strings of 1365 samples and another block after 1366 samples with the sequence repeated.) Each block is windowed with a four-term Blackman-Harris window,¹ and a single output discrete Fourier transform (DFT) is performed on the windowed block. A single complex output, the voltage, is produced every 18.2 msec for each antenna. The overlap implies that the voltages have correlated error. A maximum of 55 data samples is obtained for each target.

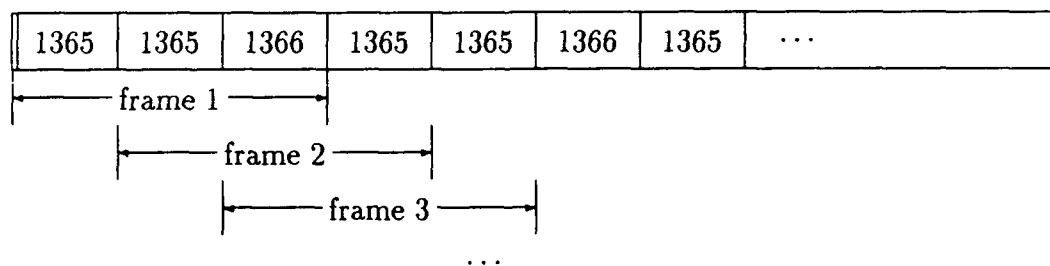


Figure 8: Schematic of data from one antenna

The noise bandwidth for each output bin of a DFT performed on 4096 samples obtained at a 75 kHz sampling rate with the 4-term Blackman-Harris window is 36.6 Hz with bin centers at intervals of 18.3 Hz, so that at worst case, a satellite could be 9.15 Hz away from bin center. The received frequency varies during a satellite pass with a typical Doppler rate

¹This windowing process reduces the side-lobe levels to -94 dB

of -20 Hz/sec. This is compensated by tuning the DF one bin below the bin in which the target was detected.

Each set of N_a complex voltages is converted to N_a phases and one representative amplitude. This comprises one *frame* of data. The full set of frames for a satellite pass is accompanied by a header frame, a set of integers representing the relative antenna strengths. The production of all of these numbers will now be described.

The reported amplitudes and antenna strengths are calculated as follows: Let

$$s_i(n) = |x| + |y| \quad \text{for } i = 1, \dots, N_a \\ \text{and } n = 1, \dots, 55,$$

where x and y are the real and imaginary parts of the complex voltage at antenna i for the n^{th} frame. The amplitude for the n^{th} frame, $S(n)$, is the olympic average² of the amplitudes at all the antennas (the $s_i(n)$), expressed in dB above 1 mW as

$$ia(n) = -[20 \log S(n) - \text{SBIAS}],$$

where $[\cdot]$ is the greatest integer function, and SBIAS is a system constant for scaling. These integers, $ia(n)$, are the amplitudes (typically they are between -160 and -118 dBm). With $S = \sum S(n)$, and $C_i = \sum_n s_i(n)$, the antenna strengths are given by

$$iant_i = \left[20 \log \frac{C_i}{S} + 32 \right],$$

limited to the range 0 to 63. The ratio C_i/S is the amplitude ratio for the i^{th} antenna, and the additive constant (32) is introduced to bias the numbers away from zero.

After these numbers have been produced, a determination is made of how many frames to send to the Operations Center: the numbers $S(n)$ are tested in reverse order until a value of $S(n)$ is above the threshold. Let

$$N_f = \max\{n : S(n) > \text{Threshold}\}.$$

The frames from 1 to N_f are transmitted.

To accomodate data transmission the phase at each antenna is quantized to 6 bits, as follows: For the first N_f frames, the receiver software converts (x, y) , the real and imaginary parts of the complex voltage, to a phase (an integer in $[0, 63]$) using

$$\bar{\phi} = \left[8 \frac{y}{x} + .5 \right] \quad \text{for } 0 \leq y \leq x.$$

²The olympic average of a set of numbers is obtained by deleting the largest and smallest numbers and taking the arithmetic mean of the remainder.

The range given covers only the first octant; the second octant is deduced from

$$\tan^{-1} z = \pi/2 - \tan^{-1} 1/z \quad \text{for } z \geq 1,$$

which yields

$$\bar{\phi} = 16 - [8\frac{x}{y} + .5] \quad \text{for } 0 \leq x \leq y.$$

The rest of the complex plane is handled with simple trigonometry. The error for the noise-free case, $e(\phi) = \bar{\phi} - 64\phi$ (ϕ in rotations), is shown as a function of $\tan^{-1} y/x = 2\pi\phi$ for the first quadrant in the plot of Fig. 9. The error function is identical in the other quadrants.

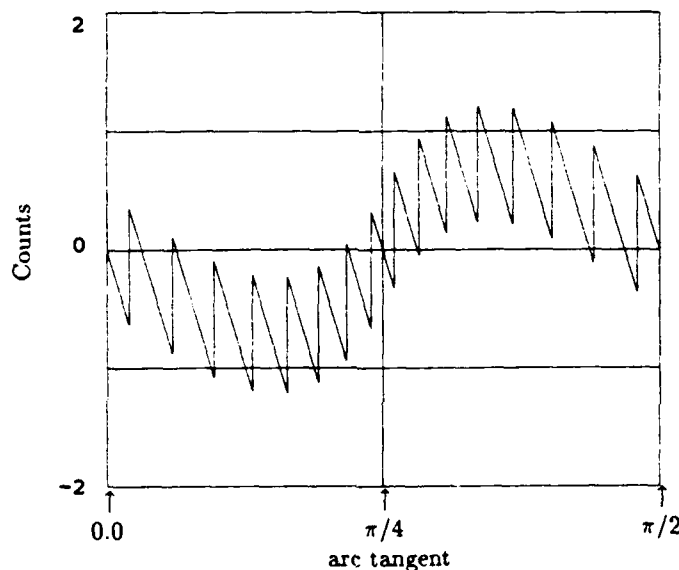


Figure 9: The phase error in the receiver software in counts, for $0 \leq \tan^{-1} y/x \leq \pi/2$.

The error is sometimes larger than one count (one count is 5.635°), even without noise.

The data sent to the ADDAS at the Operations Center begins with a header line containing the receiver doppler bin number, a set of integer antenna strengths, and a time stamp. Each data frame consists of an integer representing the amplitude and twelve integers representing the antenna phases. A typical data record is included as Table 1. The ADDAS is the interface between the telephone lines and the Operations Center computer which processes the phase data. At the Operations Center the integer phase is divided by 64, expressing the phase in rotations $\in [0, 1)$. We will use the notation $\phi_i(n)$ to mean the phase at antenna i for the n^{th} frame. At the Operations Center the iant_i are converted to amplitude ratios, wta_i , which are used as antenna weights,

$$\text{wta}_i = 10^{\text{iant}_i - 3.2}.$$

The -3.2 removes the previously applied bias.

Table 1: Typical satellite pass.

-934	34	34	31	28	32	31	30	28	34	33	32	30	890404	900110.901
-139	14	47	19	61	61	18	36	42	2	13	57	20		
-139	35	3	43	16	17	39	61	0	28	34	15	44		
-138	57	25	63	37	39	61	16	21	47	52	34	1		
-136	13	44	18	54	58	15	34	40	1	5	51	21		
-135	28	61	35	8	12	34	51	57	18	22	3	39		
-135	45	14	50	23	27	50	3	9	34	36	19	54		
-135	58	26	2	36	41	0	17	23	49	49	32	6		
-134	7	37	14	51	53	11	31	34	61	61	45	19		
-134	17	49	25	62	0	23	41	46	9	5	55	32		
-134	27	59	34	7	10	32	50	55	17	14	0	41		
-134	33	1	43	15	16	40	59	63	26	19	6	49		
-135	39	7	47	18	22	46	0	4	31	24	13	56		
-135	45	13	51	24	28	49	5	10	35	27	16	61		
-136	47	15	54	28	30	53	8	14	39	30	18	0		
-137	48	17	56	29	31	53	9	15	41	29	18	2		
-138	47	16	54	28	30	53	8	14	38	26	16	3		
-139	45	15	52	22	29	51	5	11	37	22	15	1		
-141	42	12	49	21	25	48	2	6	33	18	13	63		
-142	36	4	46	18	18	43	62	4	30	12	3	59		
-145	31	63	40	15	14	33	53	61	24	4	59	52		
-148	24	56	32	2	4	27	48	55	17	58	51	42		
-151	15	47	22	59	63	19	42	44	12	47	41	37		
-155	2	51	6	44	53	9	33	35	4	36	34	31		
-157	29	33	53	36	50	0	25	28	58	43	33	26		
-157	56	61	55	12	38	52	14	14	37	19	16	20		
-153	47	5	50	52	26	60	58	9	31	13	4	10		
-151	20	57	33	1	3	35	50	0	19	54	54	53		
-151	8	40	13	49	51	17	28	35	63	34	30	34		
-151	46	20	60	30	33	52	12	22	38	10	13	12		
-151	22	60	35	11	15	35	58	56	16	49	54	54		
-151	1	33	12	55	49	16	25	29	1	25	21	34		
-153	32	2	56	27	28	44	2	16	32	63	61	6		
-154	14	47	17	4	61	26	33	40	0	29	33	40		
-153	49	17	53	48	22	49	12	5	43	10	55	17		
-158	5	49	21	45	12	21	28	48	1	35	35	42		
-156	8	16	8	26	29	40	1	0	33	21	62	16		
-155	10	47	5	6	35	37	48	56	28	20	44	38		

3 The Observation Time

A specific frame is selected at which to base the direction cosine estimates. It is desirable that the frame (called NFT0) be at a time when the amplitude of the signal is high, and that the satellite north-south cosine be near zero. The algorithm for the selection of the frame NFT0 follows: Let the integer NF1 be the number of the frame which is the first occurrence of the highest amplitude. Integer NF2 is a weighted mid-point for the satellite pass which is defined to be the maximum M satisfying

$$\sum_{n=1}^M \text{wtf}_n < \frac{1}{2} \sum_{n=1}^{N_f} \text{wtf}_n$$

where N_f is the number of frames in the pass. The desired frame, NFT0, is the truncated average of NF1 and NF2. The observation time is the time of frame NFT0.

The weight function will be used in the phase smoothing, and is obtained in the following manner: let $ia = ia(n)$ be the amplitude for the n^{th} frame, then let

$$x = \begin{cases} 10^{-.1ia-16}, & \text{if } ia \geq -160; \\ 1 & \text{otherwise} \end{cases}$$

(x is inversely proportional to the amplitude down to -160 dBm); then the weight wtf_n for the n^{th} frame is

$$\text{wtf}_n = \frac{1}{\sum_{i=0}^5 c_i x^i + 0.0045^2}$$

where the coefficients are given by

$$\begin{aligned} c_0 &= 0.000135 \\ c_1 &= 0.016142 \\ c_2 &= 0.313793 \\ c_3 &= -1.174551 \\ c_4 &= 1.357612 \\ c_5 &= -0.374264, \end{aligned}$$

and 0.0045 is $1/64^{\text{th}}$ of $1/\sqrt{12}$, the standard deviation of the error due to 6 bit quantization of the unit interval, $[0, 1]$. The form of the weight function was determined by Mr. Richard Smith (private communication), the head of the NAVSPASUR Analysis and Software Department, since retired. He used a polynomial fit of the variance *vs.* amplitude for the data taken at the beginning of Phase 4 of the Modernized Receiver System. The weight function is shown in the plot of Fig. 10.

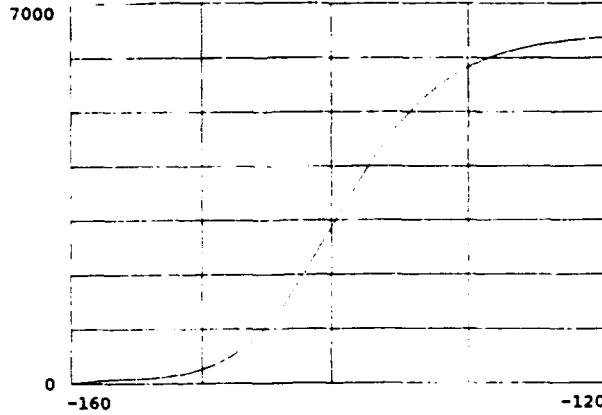


Figure 10: The weighting function of frame amplitude

4 Cosine Rates and Smoothed Phases

The center of the antenna array is selected as the reference point. An iterative, weighted least squares differential correction procedure is performed on the phase data to produce smoothed phases on all the antennas at frame NFT0, and for all the frames at the reference point (but see the next paragraph. The latter is called the *phase profile*. The differential correction also provides satellite direction cosine rates. All of this is described in this Section. The smoothed phases at the time of frame NFT0 are used to calculate the direction cosines in the next Section. The use of the phase difference profile to determine the Doppler and chirp is discussed in Section 6.

The cosine rates and smoothed phases are determined in two or three least squares iterations. As will be seen, the phase profile is not directly solved for; rather the differential correction determines the *phase difference* profile, the phase profile minus the phase at NFT0. Usually three steps are performed, but during heavy traffic, provision is made to limit the processing to two iteration steps. Also, as will be described, if after the second iteration, the estimates are good enough, there is no third iteration. The following description is summarized as the flow chart of Fig. 11.

In the first step only the phases at NFT0, $\phi_i \stackrel{\text{def}}{=} \phi_i(\text{NFT0})$, and the cosine rates are adjusted; 0.0 is used for the initial values of the cosine rates. The measured phases at all N_a antennas for all N_f frames are the observations; the calculated values from the model are given by

$$c_i(n) = \phi_i + \Delta\phi(n) + \dot{m}_1 x_i t_n + \dot{m}_2 y_i t_n,$$

where

$\phi_i = \phi_i(\text{NFTO})$ is the model phase at antenna i at the observation time,
 \dot{m}_1 and \dot{m}_2 are the east-west and north-south cosine rates,
 $\Delta\phi(n) = \phi_{\text{ref}}(n) - \phi_{\text{ref}}$ is the model phase difference profile,
 $\phi_{\text{ref}}(n)$ is the phase profile, the phase at the reference point for the n^{th} frame,
 x_i and y_i are the antenna coordinates with respect to the reference point,
 and t_n is the time difference between the n^{th} frame and NFTO.

Only the first two are adjusted in the first iteration.

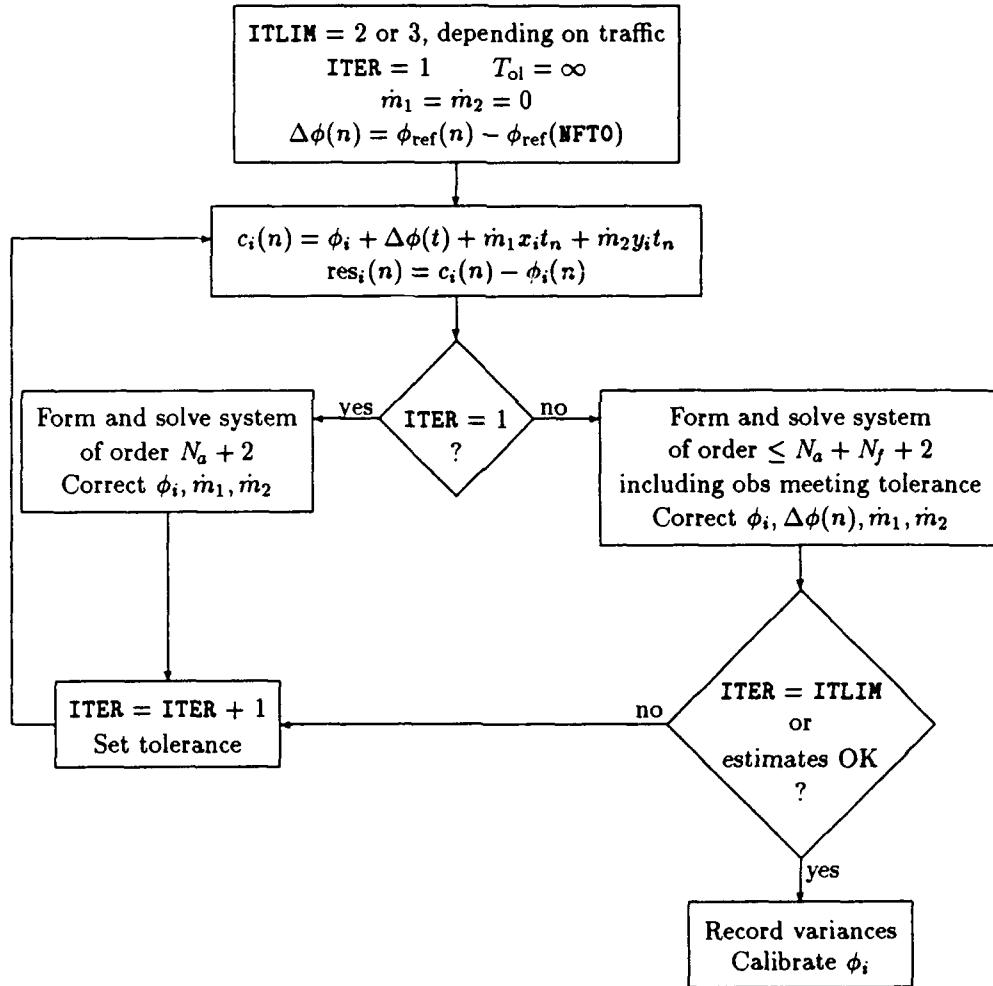


Figure 11: Flow chart summary of phase smoothing and cosine rates.

The term *least squares* means a process of minimizing a squared difference. The most common example is fitting a curve to measurements, but there are many scientific and engineering applications of the technique, which may be viewed as a generalization of the curve-fitting problem. The theory is developed in many places including pp. 123-5 of [Bate] and is summarized in an appendix.

The least squares correction process requires the solution to the equation

$$A^t W A \Delta P = A^t W (O - C),$$

where A is the matrix of partial derivatives of calculated values with respect to the parameters:

$$\frac{\partial c_i(n)}{\partial \phi_j} = \delta_{ij} \quad \frac{\partial c_i(n)}{\partial (\dot{m}_1, \dot{m}_2)} = (x_i t_n, y_i t_n).$$

A is given by

$$A = \begin{pmatrix} I_{N_a} & \vec{x}t_1 & \vec{y}t_1 \\ I_{N_a} & \vec{x}t_2 & \vec{y}t_2 \\ \vdots & \vdots & \vdots \\ I_{N_a} & \vec{x}t_{N_f} & \vec{y}t_{N_f} \end{pmatrix},$$

where I_{N_a} represents the identity matrix of order N_a , and \vec{x} and \vec{y} are the column vectors of the x and y coordinates of the antennas. The weight matrix W is diagonal with entries equal to the relative weight assigned to each observation,

$$W = \text{diag} \{ \text{wt}_{1,1}, \dots, \text{wt}_{N_a,1}, \text{wt}_{1,2}, \dots, \text{wt}_{N_a,2}, \dots, \text{wt}_{N_a,N_f} \}.$$

Here wt_{ni} is the weight assigned to the phase measurement at antenna i for frame n , and is given by the product, $\text{wtf}_n \text{wta}_i$, of the weight for frame n (determined in Section 3) and the weight for the i^{th} antenna (Section 2). ΔP is the vector of improvements to the parameters P , and $O - C$ is the vector of residuals, $\phi_i(n) - c_i(n)$, which are normalized to $[-0.5, 0.5]$ by adding or subtracting 1, which avoids the usual difficulties in unwrapping the measured phases.

The matrix $A^t W A$ is known as the inverse covariance matrix because when the weights are the reciprocals of the variances of the observations, $(A^t W A)^{-1}$ gives the covariance matrix for the new estimates. In particular, its i^{th} diagonal entry is the variance (square of the standard deviation) of the adjusted estimate of the i^{th} parameter, $P_i + \Delta P_i$.

$A^t W A$ may be expressed as a block matrix

$$A^t W A = \begin{pmatrix} m_{11} & m_{12} \\ m_{12}^t & m_{22} \end{pmatrix},$$

where m_{11} is diagonal, $N_a \times N_a$, with element ii given by $\sum_n wt_{ni}$. The $N_a \times 2$ matrix

$$m_{12} = \sum_n wt_{ni} t_n (x_i \ y_i),$$

and

$$m_{22} = \sum_i \sum_n wt_{ni} t_n^2 \begin{pmatrix} x_i^2 & x_i y_i \\ x_i y_i & y_i^2 \end{pmatrix}$$

is 2×2 .

The vector $A^t W(O - C)$ has $N_a + 2$ elements

$$\begin{pmatrix} \sum_n wt_{ni} (\phi_i(n) - c_i(n)) \\ \sum_i \sum_n wt_{ni} t_n (\phi_i(n) - c_i(n)) \begin{pmatrix} x_i \\ y_i \end{pmatrix} \end{pmatrix},$$

with the residuals, $(\phi_i(n) - c_i(n))$, normalized to $[-.5, .5]$.

The block structure of $A^t W A$ makes the matrix inversion fairly straightforward, resulting in adjustments to be made to ϕ_i and the cosine rates.

The second iteration begins with the adjusted values as well as the unadjusted history of phase differences $\Delta\phi(n)$, which are now also to be adjusted. The calculated values take the same form:

$$c_i'(n) = \phi_i + \Delta\phi(n) + \dot{m}_1 x_i t_n + \dot{m}_2 y_i t_n.$$

The matrices involved are considerably larger than on the first iteration, since there are N_f more parameters. Also, only observations meeting the tolerance, *i.e.*, that

$$wt_{ni} |\phi_i(n) - c_i(n)|^2 \leq T_{ol},$$

are included in the sums, where

$$T_{ol} = 4 \max \left\{ \frac{S_2}{N_a N_f - N_f - N_a - 2}, 1 \right\}$$

and $S_2 = \sum_i \sum_n wt_{ni} (\phi_i(n) - c_i(n))^2$ is the weighted sum of the squared residuals from the first iteration. The matrix A now includes the partial derivatives

$$\frac{\partial c_i(n)}{\partial \Delta\phi(m)} = \delta_{nm},$$

so A is given by

$$A = \begin{pmatrix} I_{N_a} & E_1 & \vec{x}t_1 & \vec{y}t_1 \\ I_{N_a} & E_2 & \vec{x}t_2 & \vec{y}t_2 \\ \vdots & \vdots & \vdots & \vdots \\ I_{N_a} & E_{N_f} & \vec{x}t_{N_f} & \vec{y}t_{N_f} \end{pmatrix},$$

where E_k is the $N_a \times N_f$ matrix whose k^{th} column is all 1s, and the other entries are 0.

The submatrix m_{11} is no longer diagonal, and now of size $N_a + N_f \times N_a + N_f$, in the form

$$m_{11} = \begin{pmatrix} \sum_n \text{wt}_{ni} & \text{wt}_{ni} \\ (\text{wt}_{ni})^t & \sum_i \text{wt}_{ni} \end{pmatrix},$$

where wt_{ni} (unsummed) represents the $N_a \times N_f$ block of individual weights. Also

$$m_{12} = \begin{pmatrix} \sum_n \text{wt}_{ni} t_n(x_i, y_i) \\ \sum_i \text{wt}_{ni} t_n(x_i, y_i) \end{pmatrix},$$

is of size $N_a + N_f \times 2$, and m_{22} is as before.

The vector $A^t W(O - C)$ has $N_a + N_f + 2$ elements

$$\begin{pmatrix} \sum_n \text{wt}_{ni} (\phi_i(n) - c_i(n)) \\ \sum_i \text{wt}_{ni} (\phi_i(n) - c_i(n)) \\ \sum_i \sum_n \text{wt}_{ni} t_n (\phi_i(n) - c_i(n)) \begin{pmatrix} x_i \\ y_i \end{pmatrix} \end{pmatrix}.$$

At the Operations Center an approximation to $A^t W A$ is made; m_{11} is taken to be diagonal:

$$m_{11} = \begin{pmatrix} \sum_n \text{wt}_{ni} & \mathbf{O}_{in} \\ \mathbf{O}_{ni} & \sum_i \text{wt}_{ni} \end{pmatrix},$$

where \mathbf{O}_{kj} represents the $k \times j$ matrix of zeroes.

If $\sum_n \text{wt}_{ni} = 0$ for some i , meaning none of the phase measured at antenna i met the tolerance, or $\sum_i \text{wt}_{ni} = 0$ for some n , meaning none of the phases measured at frame n met the tolerance, the matrix $A^t W A$ as given would be singular. Instead the system of equations is purged of the row and column containing the term.

A third iteration is made if traffic has not been too heavy, and if the dot product of the quantities $A^t W(O - C)$ and the applied correction is more than 20% of S_2 , the weighted sum of the squared residuals which met the tolerance during the second iteration. If a third iteration is to be made, a new tolerance is computed:

$$4 \max \left\{ \frac{S_2 N_f N_a}{S_0 (S_0 - N_f - N_a - 2)}, 1 \right\},$$

where S_0 is the number of observations that met the tolerance in the second iteration.

The variances, Var_i , of the estimates of ϕ_i are set to numbers proportional to the diagonal elements of $(A^T W A)^{-1}$ and recorded, so that new weights for the antennas can be used for direction cosine estimation.

The resulting phases, ϕ_i , are calibrated by subtracting the calibration phases. The adjusted (and calibrated) values will be referred to with the same symbols, ϕ_i for the N_a phases at frame NFT0 (whether normalized to $[0, 1]$ or to $[-.5, .5]$), \dot{m}_1 and \dot{m}_2 for the direction cosine rates, and $\Delta\phi(n)$ for the phase difference history at the reference antenna.

5 Direction Cosines

The walkup technique is a systematic step-by-step resolution of the direction cosine from the phase differences, beginning with an estimate due to the phase difference on the shortest baseline and adjusting the estimate in steps through sequentially longer baselines. The procedure is performed on both arms of the St. Andrew's cross to determine the direction cosines with respect to each of the arms. In this Section the theory is explained and then the implementation. The direction cosines thus determined are improved with a least squares differential correction procedure.

5.1 The Walkup Method

This algorithm has recently been modified by the Analysis and Software Department [Bales] of NAVSPASUR for use with the St. Andrew's cross configuration. Let $\bar{b}_i = b_i/\lambda$ be the i^{th} baseline (in wavelengths) in ascending order of length, and let ϕ_i be the calibrated phase difference in rotations between the phases measured on the two antennas comprising baseline \bar{b}_i . In the Operations Center software, the phase differences are normalized to $[0, 1]$, but we shall assume $\phi_i \in [-.5, .5]$, which makes the description easier. The initial estimate of the direction cosine is as given in Eq. (3): $c_1 = \phi_1/\bar{b}_1$. The iteration step of the walkup is as follows: Assume we have c_{i-1} , the cosine estimate after processing baseline $i-1$, and let $\Phi = c_{i-1}\bar{b}_i$ and $\bar{\Phi} = [\Phi] + \phi_i$. If the absolute value of $\bar{\Phi} - \Phi$ is greater than 0.5, then $\bar{\Phi}$ is adjusted toward Φ by ± 1 . The quantity $\bar{\Phi}$ is the total phase difference on baseline \bar{b}_i , composed of an integer, $[\Phi]$, and fractional part, ϕ_i . The new cosine estimate is given by $c_i = \bar{\Phi}/\bar{b}_i$.

In order that c_1 be uniquely determined from the phase difference on baseline b_1 , i.e., that there be no cosine ambiguity at the first step, it is necessary that $c_1^\pm = (\phi_1 \pm 1)\lambda/b_1$ represent

values larger than $1/\sqrt{2}$ which are unphysical, since direction cosines on the diagonal baselines are between approximately 45° and 135° . The condition is met provided $b_1 < \lambda/\sqrt{2}$. Similarly, in order to avoid an ambiguity at each step in the walkup procedure, it is necessary that the sequence of baselines (b_i) grow slowly. The error in Φ is \bar{b}_i/\bar{b}_{i-1} ($= b_i/b_{i-1}$) times the error in the phase difference, ϕ_i . The restriction that $b_i/b_{i-1} < 2$ keeps the error on Φ low enough, it is hoped, to determine the integer $[\Phi]$ correctly sufficiently often.

5.2 Implementation

Physical baselines along L_1 and L_2 do not satisfy the conditions: the shortest is $20\sqrt{2}$ feet, and there are ranges where we would have $b_i > 2b_{i-1}$. The lists of baselines for L_1 and L_2 are in the first columns in each half of Table 2. This is overcome with virtual baselines, created using second (and more) differences. For example, there are baselines along L_2 of $20\sqrt{2}$ and $44\sqrt{2}$ feet, whose phase differences can be differenced to form a virtual baseline of $24\sqrt{2}$ feet.

A virtual antenna, V1, is introduced to fill the missing corner, at the point (1200, 1200) (see Fig. 4), with a phase (in this paragraph we are using ϕ_i for the phase at antenna i rather than the phase difference on baseline b_i .)

$$\phi_{V1} = \text{fractional part}(\phi_1 + \phi_{12} - \phi_4),$$

and variance

$$\text{Var}_{V1} = \frac{1}{3}(\text{Var}_1 + \text{Var}_{12} + \text{Var}_4),$$

which may be compared with the theoretical value

$$\text{Var}_{V1} = \text{Var}_1 + \text{Var}_{12} + \text{Var}_4.$$

The L_1 baselines added with antenna V1 are shown in the second column of Table 2. Another virtual antenna, V2, is introduced at the center of the X; it will be assigned a phase equal to the average of the phases at antennas 1 and 12, *i.e.*,

$$\phi_{V2} = \frac{1}{2}(\phi_1 + \phi_{12}) \quad \text{or} \quad \phi_{V2} = \frac{1}{2}(\phi_1 + \phi_{12} + 1), \quad (4)$$

and variance

$$\text{Var}_{V2} = \frac{1}{2}(\text{Var}_1 + \text{Var}_{12}),$$

which may be compared with the theoretical value

$$\text{Var}_{V2} = \frac{1}{4}(\text{Var}_1 + \text{Var}_{12}).$$

Table 2: St. Andrew's cross baselines

L_1 Baseline	Using V1	Using V2	Using L_2	L_2 Baseline	Using V2	Using L_1
	1200			1200		
1110				1180		
1082				1136		
916				912		
888				892		
830				848		
636						
		600			600	
		510			580	
		482			536	
		406				
	370				312	
280				288		
252						
		230				
194						194
	118					
	90					
			64	64		
			44	44		
28						
			20	20		
			18			
			16			
			14			
			12			
			10			
			8			
			6			
			4			
			2			

The above are multiplied by $\sqrt{2}$

The baselines added with antenna V2 are shown in Table 2.

As indicated ϕ_{V2} is ambiguous by ± 0.5 : suppose $\phi_1 = -0.4$ and $\phi_{12} = 0.4$; then one can have $\phi_{V2} = 0.0$, but $\phi_{V2} = \pm 0.5$ is equally possible. This has assumed the ϕ_i are normalized to $[-0.5, 0.5]$, but other normalizations are analagous. Actually the ℓ_1 walkup begins without a value assigned to ϕ_{V2} . The phase differences for baselines including V2 are tentatively chosen based on whatever value ϕ_{V2} happens to have (random). Near the end of the ℓ_1 determination, ϕ_{V2} is recomputed. We will see that there is no harm in this.

A total of 42 baselines are used in the walkup, 31 for ℓ_1 and 12 for ℓ_2 . Three of the L_2 baselines are used on L_1 ; these are 20, 44, and 64 feet (times $\sqrt{2}$). If it is true that at frame NFT0, the north-south direction cosine is small, then from Eq. (1) we must have that $\ell_1 \sim \ell_2$. In this case, the phase differences which would be produced on short baselines on L_1 and L_2 will be approximately equal. This is the justification for using short L_2 baselines as if they were along L_1 . As will be seen the rather longer L_1 baseline of $194\sqrt{2}$ is used for the first ℓ_2 walkup step. The last columns in each half of Table 2 show the baselines contributed through the use of L_1 and L_2 baselines (and virtual baselines) on L_2 and L_1 .

The algorithm for determining the direction cosines from the smoothed phases at the reference time (frame NFT0), as described in the rest of this Subsection, is summarized as the flow chart of Fig. 12. The list of the phase differences used for the baselines is shown in Table 3, where the common factor of $\sqrt{2}$ has been suppressed. The shortest baseline used in NAVSPASUR direction cosine processing is $2\sqrt{2}$ feet which is sufficient to avoid a cosine ambiguity at the first step, i.e., satisfies the condition $b_1 < \lambda/\sqrt{2}$, since λ is more than 4 feet. With this set of baselines on L_1 , we have $b_i < 2b_{i-1}$ except for the shortest pair of baselines.

The cosine on L_1 , ℓ_1 , is determined by walkup through all baselines indicated in the Table (The ones up to $194\sqrt{2}$ inclusive are independent of ϕ_{V2}), testing each successive estimate. If

$$|c_i - c_{i-1}| > .25/\bar{b}_i,$$

then a weighted least squares estimate is performed (as described in the next Subsection) on the baselines and phases up to i (but not including the ones that depend on ϕ_{V2}) to redetermine c_i , using c_{i-1} as the initial estimate. Since ϕ_{V2} has not yet been chosen (see above), baselines dependent on ϕ_{V2} , c_i will include a random error, which is likely to trigger the least squares process to recalculate c_i without using baselines dependent on ϕ_{V2} .

After the walkup has proceeded through the longest L_1 baseline, regardless of whether the resulting c_i meets the $0.25/\bar{b}_i$ tolerance, a least squares fit is performed for ℓ_1 using baselines independent of ϕ_{V2} . This allows a determination of ϕ_{V2} , choosing from Eq. (4) the value for ϕ_{V2} whose phase difference with respect to antenna 4 (see Fig. 4) most closely

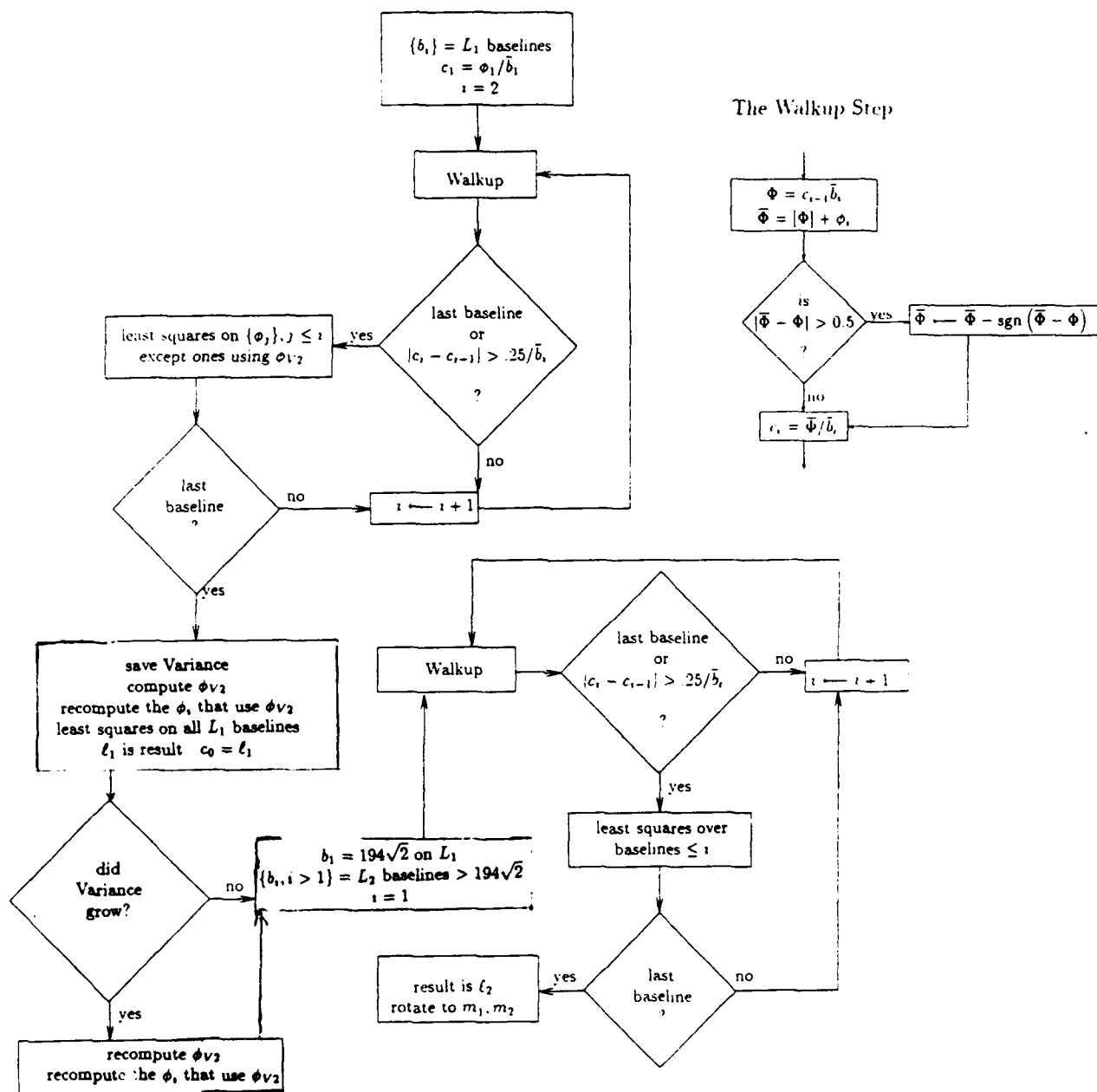


Figure 12: Flow chart summary of direction cosine resolution

Table 3: Antenna pairs used to create baselines

L_1 Baseline	Antennas	L_2 Baseline	Antennas
1200	V1-4	1200	12-1
1110	9-4	1180	11-10
1082	8-4	1136	10-1
916	9-5	912	12-6
888	8-5	892	11-6
830	7-4	848	10-6
636	7-5	600	12-V2
600	V2-4	580	11-V2
510	9-V2	536	10-V2
482	8-V2	312	V2-6
406	V2-5	288	6-1
370	V1-7	194	5-4
280	9-7	64	12-10
252	8-7	44	11-10
230	7-V2	20	12-11
194	5-4		
118	V1-8		
90	V1-9		
64	12-10		
44	11-10		
28	9-8		
20	12-11		
18	11-10 V1-9 12-10		
16	11-10 9-8		
14	12-10 V1-9 12-11*		
12	12-11 12-10 11-10 9-8		
10	9-8 11-10 V1-9 12-10		
8	9-8 12-11		
6	V1-9 12-10 12-11		
4	12-11 11-10 9-8		
2	12-10 V1-9 9-8		

* The $20\sqrt{2}$ foot baseline is used twice.

matches the phase difference calculated for a $600\sqrt{2}$ foot L_1 baseline. The phase differences which use ϕ_{V2} are recomputed. Provision is made for a final least squares fit to be performed on ℓ_1 , this time using all the baselines. The final least squares fit on ℓ_1 is not done if the penultimate estimate is considered adequate. See the next Subsection.

This final value of ℓ_1 is used as the starting value for ℓ_2 , on which a walkup is performed, first to the $194\sqrt{2}$ foot baseline of L_1 , and then on longer L_2 baselines. A least squares fit is performed on ℓ_2 . Finally, these values are rotated back into north-south and east-west components using Eq. (1).

5.3 Least Squares Adjustment

During the processing described in the previous Subsection, the direction cosines ℓ_1 and ℓ_2 are corrected with a least squares fit to the phase differences ϕ_i using $\phi_i = \ell_j \bar{b}_i$ (derived from Eq. (3)) as the model. The partial derivatives involved are

$$\frac{\partial \phi_i}{\partial \ell_j} = \bar{b}_i.$$

Since there is only one parameter being adjusted (ℓ_1 and ℓ_2 are handled separately) the differential corrections to ℓ_1 and ℓ_2 are the solutions, $\Delta \ell_1$ and $\Delta \ell_2$, of scalar equations and given by:

$$\Delta \ell_j = \frac{\sum w t b_i \bar{b}_i (\phi_i - \bar{b}_i \ell_j)}{\sum w t b_i \bar{b}_i^2}, \quad (5)$$

where $j = 1, 2$ and the sums run over the baselines used.

There is no tolerance test for the residuals in the least squares, but not all of the baselines are used. During the ℓ_1 walkup, if a least squares fit is performed for L_1 baselines up to (and including) $194\sqrt{2}$ feet (this happens, for example if $|c_i - c_{i-1}| > .25/\bar{b}_i$), all baselines up to the present one are considered, including the three short L_2 baselines and all the virtual baselines (from $2\sqrt{2}$ to $18\sqrt{2}$ feet). For walkup on longer baselines, the shortest nine and the L_2 baselines are excluded, so it starts with $28\sqrt{2}$; it does not use the ones that use ϕ_{V2} . After the first least squares for the $1200\sqrt{2}$ -foot baseline (which does not include the L_2 or ϕ_{V2} baselines), then a test is made. If

$$\frac{\frac{1}{N_b} \sum w t b_i (\phi_i - \bar{b}_i \ell_j)^2}{\sum w t b_i \bar{b}_i^2} < 10^{-7}, \quad (6)$$

where N_b is the number of baselines involved in the least squares (14 in this case), then the new value, $\ell_1 + \Delta \ell_1$, is accepted, and there is no final least squares step for ℓ_1 . If the

inequality does not hold, then after the final least squares step for ℓ_1 , the left hand side of Eq. (6) is recomputed. The numerator is the sample variance of the previous estimate of ℓ_1 , and the denominator is the theoretical variance of the new estimate. The final (extra) least squares correction step of ℓ_1 (if performed) includes the baselines which use ϕ_{v2} , it having been determined in the meantime. During ℓ_2 , including its final least squares correction step, if the walkup step requires least squares, all baselines on L_2 (up to the present one) are used.

The weight, wtb_i , for the baseline b_i is determined from the variances, Var_{a1} and Var_{a2} , of the (real or virtual) antennas, $a1$ and $a2$, comprising b_i :

$$wtb_i = 1 / (Var_{a1} + Var_{a2}).$$

The virtual baselines are assigned weights equal to the sum of the weights of the baselines comprising the virtual baselines, except that the baseline of length $12\sqrt{2}$ feet gets the weight

$$wt_{12} = wt_{28} + \frac{1}{3} (wt_{20} + wt_{44} + wt_{64}),$$

where the subscripts identify the baseline length (except for the $\sqrt{2}$). The $14\sqrt{2}$ feet baseline includes the $20\sqrt{2}$ feet baseline twice, so its weight is added twice in the sum for the weight of the virtual baseline.

For the weights assigned to virtual baselines to be mathematically consistent with those of physical baselines, one would use the inverse of the sum of the variances of all of the antennas involved.

5.4 Data Quality Check

Before continuing to the Doppler and chirp processing, the quantity in Eq. (6) is tested. If it is more than $10^{-8.1}$, the cosine determination is assumed to have failed. It is possible that after the first least squares fit of ℓ_1 on the $1200\sqrt{2}$ foot baseline, the inequality in Eq. (6) holds, so that a final least squares fit for ℓ_1 is not made, but that the left hand side is larger than $10^{-8.1}$, so that the direction cosine resolution is considered failed.

6 Doppler and Chirp

A 512-point FFT is applied to an array containing the cosine and sine of

$$2\pi(\Delta\phi(n) - \Delta\phi(n-1)),$$

the increments of the phase history determined in Section 4, weighted by

$$\frac{\text{wtf}_n \text{wtf}_{n-1}}{\text{wtf}_n + \text{wtf}_{n-1}}.$$

The resulting power spectrum is smoothed with 3-point triangular smoothing:

$$P_i \Leftarrow .22 (P_{i-1} + 2.545 P_i + P_{i+1}),$$

and C_0 is chosen as the bin number of the peak power (only indices 497–512, and 1–48 are checked), adjusted somewhat by the strengths of the neighbor bins. Then a 64-point FFT is applied to the array consisting of the cosine and sine of

$$2\pi (\Delta\phi(n) - .5 C_0 t_n^2),$$

weighted by wtf_n , and the power spectrum is smoothed. The bin number of the peak is chosen as D_0 .

The values D_0 and C_0 just determined are used as initial values of the differential Doppler and chirp for a least squares estimate best fitting the phase difference history, $\Delta\phi(n)$. The calculated values are given from the model as

$$c(n) = \Delta\phi + D t_n + \frac{1}{2} C t_n^2,$$

with $\Delta\phi$ initially $\Delta\phi(0)$, the adjusted phase difference profile value at frame NFO from Section 4, and D and C the differential Doppler and chirp, initially D_0 and C_0 . The partial derivatives are

$$\frac{\partial c(n)}{\partial \Delta\phi} = 1 \quad \frac{\partial c(n)}{\partial D} = t_n \quad \frac{\partial c(n)}{\partial C} = \frac{1}{2} t_n^2.$$

These form the n^{th} row of the matrix A . The normal equation is then

$$\sum \text{wtf}_n \begin{pmatrix} 1 & t_n & \frac{1}{2} t_n^2 \\ t_n & t_n^2 & \frac{1}{2} t_n^3 \\ \frac{1}{2} t_n^2 & \frac{1}{2} t_n^3 & \frac{1}{4} t_n^4 \end{pmatrix} \begin{pmatrix} \Delta\Delta\phi \\ \Delta D \\ \Delta C \end{pmatrix} = \begin{pmatrix} \sum \text{wtf}_n (\Delta\phi(n) - c(n)) \\ \sum \text{wtf}_n t_n (\Delta\phi(n) - c(n)) \\ \frac{1}{2} \sum \text{wtf}_n t_n^2 (\Delta\phi(n) - c(n)) \end{pmatrix},$$

where the sums run over n . The first iteration is carried out without a tolerance requirement for the residuals. For the second iteration only observations meeting the tolerance

$$\text{wtf}_n(\Delta\phi(n) - c(n))^2 < T_{01}$$

are allowed, where

$$T_{01} = 4 \max \left\{ \frac{S_2}{N_f - 3}, 1 \right\},$$

and S_2 is the weighted sum of the squared residuals from the first iteration.

After the second iteration, if the dot product of the quantities $A^t W(O - C)$ and the applied correction is more than 20% of S_2 , the weighted sum of the squared residuals which met the tolerance during the second iteration, a third iteration is made, with a new tolerance:

$$T_{01} = 4 \max \left\{ \frac{S_2 N_f}{S_0 (S_0 - 3)}, 1 \right\},$$

where S_0 is the number of observations that met the tolerance in the second iteration.

The final value of D is multiplied by the sample rate and added to the receiver bin center frequency to yield the Doppler. The chirp is C times the square of the sample rate.

The bin sizes for Doppler and chirp (before the triangular smoothing) are 0.86 Hz and 5.9 Hz/sec, respectively, with ranges of ± 27.5 Hz and $[-94.5, 284.6]$ Hz/sec, respectively.

Acknowledgements

The author wishes to acknowledge helpful conversations with Emory Bales, Bill Vilkas, and Dick Smith, as well as the support of Carl Morris, Steve Knowles, and Jim Wadiak.

A Least Squares

The term *least squares* is used to mean any process of minimizing a squared difference. The best known example is fitting a curve to measurements, but there are many scientific and engineering applications of the technique, which may be viewed as a generalization of the curve-fitting problem. The theory is developed in many places including pp. 123-5 of [Bate], and will not be repeated here. We now summarize the method (and standardize the notation):

We are given a set of parameters $\{P_j\}$, which are to be improved or determined from consideration of a set of observations $\{O_i\}$. In the usual case there are more observations than parameters. The model is a functional relationship (or "fit") $O = f(P)$, so form the calculated values, $C_j = f_j(P_i)$, and let A be the matrix of partial derivatives:

$$A_{ij} = \frac{\partial f_j}{\partial P_i},$$

and let the weight matrix W be the diagonal matrix whose elements are the weights assigned to each observation. The theory says that P can be improved to $P + \Delta P$ where ΔP is the solution of the normal equation

$$A^t W A \Delta P = A^t W (O - C).$$

In terms of matrix elements, we have

$$(A^t W A)_{ij} = \sum_{\text{obs}} \frac{\partial f}{\partial P_i} \frac{\partial f}{\partial P_j} \text{weight}_{\text{obs}},$$

and the right hand side is given by

$$(A^t W (O - C))_j = \sum_{\text{obs}} \frac{\partial f}{\partial P_j} \text{weight}_{\text{obs}} (O - C).$$

The matrix $A^t W A$ is known as the inverse covariance because $(A^t W A)^{-1}$ gives the covariance matrix for the new estimates. In particular, its i^{th} diagonal entry is the variance (square of the standard deviation) of the estimate of the i^{th} parameter.

References

- [Bales] Emory H. Bales, "A Resolution Algorithm for the St. Andrew's Cross Naval Space Surveillance Center," March, 1989.
- [Bate] Roger R. Bate, Donald D. Mueller, and Jerry E. White, *Fundamentals of Astrodynamics*, Dover, 1971.
- [Kraus] J. D. Kraus, *Radio Astronomy*, McGraw-Hill, 1966.
- [Tho] A. Richard Thompson, James M. Moran, and George W. Swenson Jr., *Interferometry and Synthesis in Radio Astronomy*, Wiley, 1986.